

apparently due to the opposing effects of activation and subsequent degradation of coagulation factors. In a search for factors that may be useful for predicting an individual patient's response to heparin, baseline APTT has emerged as the variable which consistently correlates positively with slope value (4, 5, 8). Unlike humans, rats exhibit a negative correlation between baseline APTT and slope value. The reason for this species difference is not known.

In summary, coagulation studies in rats require considerably more attention to the control of the variables examined in this investigation than do similar studies in humans. The volume of blood required to determine baseline APTT and slope represents a significant fraction of a rat's total blood volume, but is negligible compared with the human blood volume. This is an additional complicating factor in studies on rats. The observed species variation may, however, be useful for exploring various aspects of the blood coagulation process. Parallel and coordinated studies on humans and rats, and perhaps also on other species, may facilitate the elucidation of important pharmacokinetic and pharmacodynamic aspects of the anticoagulant action of heparin.

REFERENCES

- (1) L. B. Jaques and L. W. Kavanagh, *Thromb. Diath. Haemorrh. (Stuttg.)*, **Suppl.**, **56**, 171 (1973).
- (2) L. B. Jaques, L. W. Kavanagh, and S. H. Kuo, *Thromb. Res.*, **3**, 295 (1973).
- (3) H. B. Nader, H. K. Takahashi, and J. A. Guimarães, *Int. J. Biol. Macromolec.*, **3**, 356 (1981).
- (4) L. R. Whitfield and G. Levy, *Clin. Pharmacol. Ther.*, **28**, 509 (1980).

- (5) L. R. Whitfield, J. J. Schentag, and G. Levy, *Clin. Pharmacol. Ther.*, **32**, 503 (1982).
- (6) J. Hirsh, W. G. van Aken, A. S. Gallus, C. T. Dollery, J. F. Cade, and W. L. Yung, *Circulation* **53**, 691 (1973).
- (7) R. J. Cipolle, R. D. Seifert, B. A. Neilan, D. E. Zaske, and E. Haus, *Clin. Pharmacol. Ther.*, **29**, 387 (1981).
- (8) T. D. Bjornsson and K. M. Wolfram, *Ann. N.Y. Acad. Sci.*, **370**, 656 (1980).
- (9) H. N. Teien and U. Abildgaard, *Thromb. Haemostas. (Stuttg.)*, **35**, 592 (1976).
- (10) W. B. Forman and G. Bayer, *Am. J. Hematol.*, **11**, 277 (1981).
- (11) T. D. Bjornsson and G. Levy, *J. Pharmacol. Exp. Ther.*, **210**, 237 (1979).
- (12) L. R. Whitfield and G. Levy, *Thromb. Res.*, **21**, 681 (1981).
- (13) R. R. Sokal and F. J. Rohlf, "Biometry," W. H. Freeman, San Francisco, Calif., 1969, p. 450.
- (14) R. R. Proctor and S. I. Rapaport, *Am. J. Clin. Path.*, **36**, 212 (1961).
- (15) J. R. Weeks and J. D. Davis, *J. Appl. Physiol.*, **19**, 540 (1964).

ACKNOWLEDGMENTS

Supported in part by Grant GM 20852 from the National Institute of General Medical Sciences, National Institutes of Health, by Biomedical Research Support Grant 2S07RR05454-19, and by a Graduate Fellowship from the State University of New York for L.R.W.

The previous (fourth) part of this series was L. R. Whitfield, J. J. Schentag, and G. Levy, *Clin. Pharmacol. Ther.*, **32**(5), 503 (1982).

Distribution and Elimination of Poly(methyl methacrylate) Nanoparticles After Subcutaneous Administration to Rats

JÖRG KREUTER *^x, M. NEFZGER †, E. LIEHL ‡, R. CZOK ‡, and R. VOGES §

Received June 14, 1982, from the *School of Pharmacy, Federal Institute of Technology, CH 8092 Zurich, Switzerland, †SANDOZ Forschungsinstitut, A 1235 Vienna, Austria, and ‡SANDOZ LTD., CH 4002 Basle, Switzerland. Accepted for publication August 25, 1982.

Abstract □ Poly(methyl [1-¹⁴C]methacrylate) nanoparticles were injected subcutaneously into rats. Almost all of the radioactivity stayed at the injection site. After an initial urinary and fecal excretion of ~1% of the administered dose per day, the rate of elimination dropped to a low level (~0.005%/day *via* the feces and ~0.0005%/day *via* the urine) within 70 days. After 200 days, the fecal elimination increased exponentially until a >100-fold increase was observed after 287 days in one rat. After this time, a tendency for an increase in fecal elimination was also observed in the other animals, and the radioactivity in all organs and tissue increased by ~100 times in all animals in comparison with the organ radioactivity determinations at earlier times.

Keyphrases □ Poly(methyl methacrylate)—¹⁴C-labeled nanoparticles, distribution and elimination in rats, subcutaneous administration □ Distribution—¹⁴C-labeled poly(methyl methacrylate) nanoparticles, subcutaneous administration in rats □ Elimination—¹⁴C-labeled poly(methyl methacrylate) nanoparticles, subcutaneous administration in rats

Poly(methyl [1-¹⁴C]methacrylate) nanoparticles were shown to be promising adjuvants for vaccines (1-4). In contrast to the rapidly biodegradable cyanoacrylates, they achieve a good adjuvant effect. The reproducibility of the adjuvant effect was much better than that of the presently

widely used aluminum hydroxide (5). Moreover, in preliminary experiments (2), poly(methyl [1-¹⁴C]methacrylate) nanoparticles seem to cause much milder tissue reactions than aluminum hydroxide.

However, the distribution and elimination of these nanoparticles after subcutaneous administration so far has not been studied. In a previous study (6) concerning the fate of poly(methyl [1-¹⁴C]methacrylate) nanoparticles after intravenous administration, a strong affinity of the nanoparticles to the reticuloendothelial system, especially to the liver, was observed.

The elimination of radioactivity after implantation of poly(methyl [1-¹⁴C]methacrylate) films was investigated in two studies (7, 8). In one study (7), an elevated elimination rate of radioactivity was observed in the urine between 2 and 8 weeks, decreasing to minimal values after this time. This elimination was probably caused by residual monomers or low-molecular weight components present in the polymer films. After 54 weeks, however, considerable radioactivity suddenly started to be eliminated (8), indicating a degradation of the polymer. This study investigates the elimination pattern and distribution

¹ Unpublished observation.

Table I—Total Radioactivity Found after 287 Days in Percent of the Administered Dose

Animal No.	903	906	910	912
Sex	M	M	M	F
Weight at start of study, g	197	207	173	206
Weight at end of study, g	574	490	458	262
Virus	- ^a	- ^a	+ ^b	+ ^b
Injection site	69.4	71.1	61.9	55.4
Excreted <i>via</i> urine (within 7 days)	6.4 (5.7)	6.2 (5.8)	6.5 (6.1)	6.8 (6.5)
Excreted <i>via</i> feces (within 7 days)	7.1 (4.9)	6.9 (4.8)	24.9 (4.5)	6.9 (4.5)
Residual body (estimated)	3–11	5–11	4–14	3–9
Total	86–94	89–95	97–107	72–78

^a No virus present in the injected sample. ^b Inactivated influenza virions present in the injected sample.

of radioactivity in the body after subcutaneous administration of poly(methyl methacrylate) nanoparticles.

EXPERIMENTAL

Preparation of Poly(methyl [1-¹⁴C]methacrylate) Nanoparticles—Methyl [1-¹⁴C]methacrylate was prepared in a three-step reaction sequence starting from barium [¹⁴C]carbonate. Carboxylation of isopropylmagnesium iodide, bromination of the resulting [1-¹⁴C]isobutyric acid, and subsequent methanolysis gave methyl 2-bromo[1-¹⁴C]isobutyrate (9). Hydrogen bromide elimination in 1,5-diazabicyclo[5.4.0]-undec-5-ene at 110° led to methyl [1-¹⁴C]methacrylate, which was continuously removed from the reaction mixture by a slow stream of helium, and collected at -196°. The ester was vacuum-transferred into phosphate-buffered saline to give a 0.5% solution. The chemical identity and chemical and radiochemical purity (>95%) were confirmed by GC after ether extraction.

The monomeric methyl [1-¹⁴C]methacrylate saline solution was used for the preparation of two nanoparticle suspensions, with and without influenza virions, for subcutaneous administration. The nanoparticles were produced by γ -irradiation-initiated polymerization with 500 krad (2.2 krad/min) in a ⁶⁰Co-source. Thus, the following suspensions were obtained:

1. Polymerization in the presence of influenza virions afforded a 0.35% suspension at a specific activity of $(5.30 \pm 0.82) \times 10^8$ dpm/ml in which all virions were incorporated into the nanoparticles.

2. Polymerization in the absence of influenza virions afforded a 0.35% suspension of virus-free nanoparticles at a specific activity of $(5.22 \pm 0.46) \times 10^8$ dpm/ml.

That the nanoparticles tended to flocculate led to difficulties in the reproducibility of the radioactivity measurements and the determination of the exact amount of the administered nanoparticles. Although the suspensions were permanently stirred during sampling of the aliquots for calibration or administration, the relative standard deviations were 14% for 0.1-ml samples of the virus-free nanoparticle suspension (26 determinations) and 9% for 0.1-ml samples containing the virion-incorporated nanoparticles (14 determinations). The addition of substituted methyl cellulose² as a stabilizer did not reduce the variation. The previously used technique of freeze-drying the suspensions (6) to obtain a homogeneous distribution of radioactivity within the resulting nanoparticle powder was not applicable because the virions would have been destroyed by this technique.

Although the animals obtained a fivefold higher volume than that used for calibration, similar variations in the dose actually administered have to be taken into consideration. Nevertheless, the material balance (the mean from the calibration experiments) is satisfactory (Table I). Since no apparent differences in the distribution and elimination of the nanoparticle preparations could be observed, both preparations were treated together as one set of data.

Excretion and Tissue Distribution after Subcutaneous Administration—A 0.5-ml aliquot of the thoroughly stirred suspension was subcutaneously injected into the neck of Sprague-Dawley rats, weighing 170–207 g, at the beginning of the study. One group of five male and five female rats received the virus-containing preparation and a second group of the same composition received the preparation with virus-free nano-

particles. The animals were kept in metabolism cages and had free access to water and food.

The elimination of radioactivity of two animals per group was measured in urine and feces up to 287 days after administration. For the determination of radioactivity in the organs, two animals per group were sacrificed at 15, 45, 66, 157, and 287 days after dosing.

Urine was collected separately from feces and stored at ~-60°. The storage container contained 100 μ l of diethylamine to maintain the urine at a pH \geq 9, thus ensuring the binding of the radioactivity excreted as carbonate. After each collection period, the cage was rinsed with water (30–40 ml) to wash out dried urine residues. The collected feces were homogenized with approximately the same weight of water. Three samples (200–400 mg) of each homogenate were analyzed.

The radioactivity in the organs was measured after sacrificing the animals by an ~0.5 ml ip injection of euthanasia solution³. From the adrenal glands, epididymis, ovary, thyroid gland, lymph nodes, and bone marrow one sample of 7–130 mg was taken; from the other organs two samples of 50–400 mg each were taken. At the application site, remaining depots were dissected and combusted⁴. The resulting carbon dioxide was absorbed in a mixture of absorber solution and scintillation cocktail⁵ and diluted up to 100 times before counting with the same mixture.

The radioactivity of the excreta, blood, plasma, and organs was determined after predrying and combustion in oxygen using a sample oxidizer (recovery of radioactivity 92–100%). The resulting [¹⁴C]carbon dioxide was absorbed in the aforementioned scintillation cocktail. The samples were then counted in a liquid scintillation counter for 20 min. The counting efficiency was determined by the external standard method; the detection limit was 4 ng/g for the bone marrow, lymph nodes, and thyroid gland and 2 ng/g for all other organs and tissue.

RESULTS AND DISCUSSION

The organ and tissue distribution after subcutaneous administration of the poly(methyl [1-¹⁴C]methacrylate) nanoparticles is shown in Table II. With the exception of the injection site, <0.1% of the administered dose could be found in the rest of the body within 15 and 157 days. The major amount of the radioactive material remained at the injection site (Tables I and III), where a hard yellow disk, ~5 mm, was found. The formation of this disk is probably caused by encapsulation with collagenous tissue, which represents the normal reaction of the body (10–12). Even after 287 days, 55–71% of the administered dose remained at the site of injection. This finding confirms previous macroautoradiographic studies in mice, in which radioactivity was detectable only at the injection site for 70 days.

In the rest of the body, the highest amounts of radioactivity were observed in the liver, spleen, lymph nodes, bone marrow, renal fatty tissue, skin, and pancreas. The comparatively high radioactivity levels in the liver, spleen, and bone marrow were not unexpected, since this was also

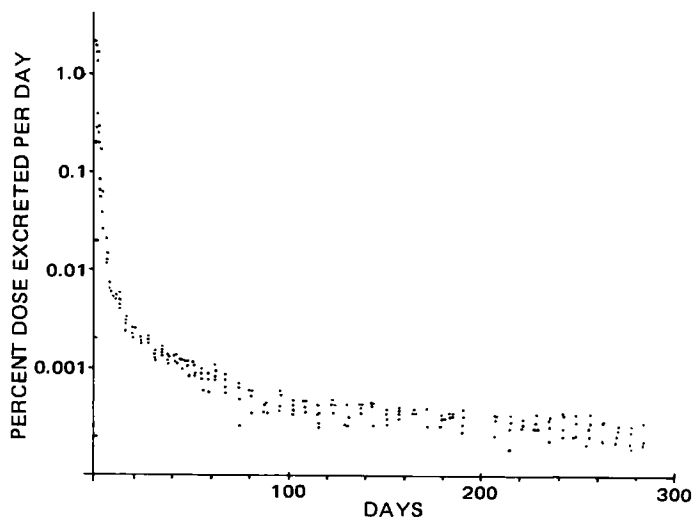


Figure 1—Rate of urinary excretion of ¹⁴C-radioactivity after subcutaneous injection of poly(methyl [1-¹⁴C]methacrylate) nanoparticles into rats (n = 4).

³ T61; Farbwerke Hoechst, Frankfurt/Main, West Germany.

⁴ Sample Oxidizer; Packard Instrument, Downers Grove, Ill.

⁵ Carbosorb and Permafluor; Packard Instrument, Downers Grove, Ill.

² Tylose MH 1000; Kalle & Co., Wiesbaden-Biebrich, West Germany.

Table II—Distribution of ¹⁴C-Radioactivity in Organs after Subcutaneous Administration of ¹⁴C-Labeled Poly(methyl methacrylate) Nanoparticles to Rats ^a

Organ or Tissue	Days				
	15	45	66	157	287
Blood	4.5 ± 1.5	1.6 ± 0.6	0.2 ± 0.4	0.4 ± 0.5	107.4 ± 108.5
Plasma	— ^b	—	—	—	114.4 ± 167.0
Liver	8.2 ± 6.2	1.9 ± 0.4	3.1 ± 3.7	1.2 ± 0.8	255.3 ± 220.7
Spleen	3.7 ± 2.7	2.7 ± 1.3	10.9 ± 13.4	2.9 ± 3.3	122.6 ± 106.8
Pancreas	2.9 ± 1.0	2.0 ± 0.9	1.5 ± 0.6	—	605.5 ± 418.1
Kidneys	4.1 ± 0.7	1.4 ± 0.4	0.7 ± 0.3	—	104.0 ± 72.3
Adrenals	—	—	—	—	244.9 ± 215.0
Fatty renal tissue	4.3 ± 1.6	2.8 ± 1.0	1.8 ± 0.9	—	461.6 ± 102.6
Testes	1.6	—	—	—	40.0 ± 21.4
Uterus	—	—	—	—	56.4
Epididymis	1.6	—	—	—	109.0 ± 73.2
Ovary	1.6	—	—	—	115.7
Colon	1.8 ± 1.0	1.7 ± 0.6	0.8 ± 1.0	—	79.3 ± 18.4
Stomach	1.1 ± 0.5	—	—	—	51.5 ± 25.2
Small intestine	2.6 ± 0.4	1.1 ± 0.5	0.6 ± 0.1	0.4 ± 0.3	84.4 ± 42.8
Salivary glands	—	—	—	—	119.2 ± 76.0
Lymph nodes	6.8 ± 10.0	6.6 ± 7.3	543 ± 812	—	277.0 ± 55.2
Thyroid glands	—	—	—	—	153.2 ± 59.8
Lungs	3.2 ± 1.0	1.4 ± 0.6	0.7 ± 0.3	—	28.1 ± 19.8
Heart	1.8 ± 1.0	0.7 ± 0.2	0.4 ± 0.3	—	96.5 ± 44.8
Muscles	1.7 ± 0.3	1.2 ± 0.3	0.6 ± 0.1	—	105.5 ± 6.1
Bone marrow	—	—	—	—	847.4 ± 197.9
Skin	4.7 ± 2.1	3.1 ± 0.5	2.2 ± 0.7	—	205.4 ± 48.3
Brain	0.9 ± 0.4	—	—	—	90.0 ± 28.6

^a Mean (ng/g) ± SD; n = 4. Administered dose = ~8 mg/kg. ^b — Less than the detection limit (<4 ng/g for bone marrow, lymph nodes, and thyroid; <2 ng/g for all other organs and tissues).

Table III—Residual Radioactivity at the Injection Site in Percent of the Injected Dose

Days	Samples without Virus		Samples with Virus	
	15	41.5	41.7	56.2
45	79.1	74.0	49.5	55.2
66	59.0	91.8	65.3	55.2
157	88.3	76.1	68.6	68.6
287	69.4	71.1	61.9	55.4

seen after intravenous administration. In contrast to the intravenous study, the radioactivity in the lymph nodes was high in some cases.

The radioactivity in the organs decreased from day 15 until day 157. Between day 157 and day 287, a sudden ~100-fold increase in radioactivity occurred in all organs of all animals. The ratio of blood radioactivity to organ radioactivity, however, remained largely unaltered (Table IV). This indicates that nanoparticles or their degradation products were transported *via* the blood.

Table IV—Ratio of Organ Radioactivity to Blood Radioactivity

Organ or Tissue	Days				
	15	45	66	157	187
Plasma	0.15	— ^a	—	—	0.79
Liver	—	1.36	16.08	3.48	3.58
Spleen	1.13	1.85	60.93	6.35	1.78
Pancreas	0.70	1.26	5.91	—	8.47
Kidneys	0.97	0.92	2.51	—	1.39
Adrenals	—	—	—	—	2.91
Fatty renal tissue	1.08	1.82	6.66	—	7.92
Testes	0.37	—	1.44	—	0.56
Uterus	—	—	—	—	0.89
Epididymis	0.41	—	2.50	—	1.41
Ovary	0.29	—	—	—	1.83
Colon	0.43	1.01	2.83	—	1.42
Stomach	0.27	—	1.64	—	0.77
Small intestine	0.65	0.68	1.98	2.36	1.25
Salivary glands	—	—	1.54	—	1.60
Lymph nodes	1.47	4.09	3174.50	—	5.90
Thyroid glands	—	—	2.63	—	2.32
Lungs	0.89	0.82	2.57	—	0.72
Heart	0.45	0.34	1.13	—	1.56
Muscles	0.43	0.71	2.32	—	2.06
Bone marrow	—	—	13.48	—	16.22
Skin	1.36	2.03	8.97	—	3.38
Brain	0.25	—	1.40	—	1.66

^a — Radioactivity in the tissue below the detection limit.

The excretion of the radioactivity in the urine of four rats is shown in Fig. 1; the excretion in the feces is shown in Fig. 2. Initially, the excretion of radioactivity was rapid: approximately 1% of the administered dose was excreted per day in the urine, with approximately the same amount excreted in the feces. Consequently, ~6% of the dose was eliminated *via* the urine and 5% *via* the feces within 7 days. However, the excretion rate dropped very rapidly until a very slow constant logarithmic decline of the excretion rate was reached after ~70 days. At this stage, only ~0.005% of the administered dose was eliminated per day, mainly *via* the feces ($t_{1/2}$ ~ 140 days) where the level of excretion was ~10 times higher than in the urine ($t_{1/2}$ ~ 170 days). After ~200 days, however, the rate of excretion started to increase continuously in one rat until a >100-fold increase was reached after 287 days. At this stage, the elimination rate amounted to 1% of the administered dose per day. A tendency for an increase in the excretion rate also could be observed in the three other animals at the end of the observation period.

The observed increases in the excretion rate do not seem to be coincidental, since they were accompanied by the aforementioned 100-fold increase in the radioactivity level of all organs in all four rats. The ob-

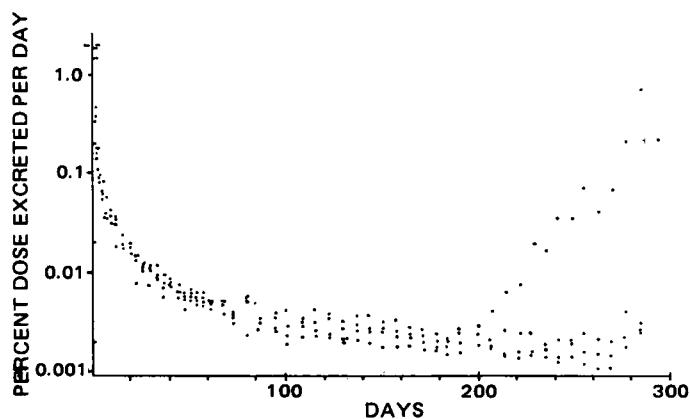


Figure 2—Rate of fecal excretion of ^{14}C -radioactivity after subcutaneous injection of poly(methyl $[1-^{14}\text{C}]$ methacrylate) nanoparticles into rats ($n = 4$).

ervation of a lag phase for the elimination of implanted material is not new. In 1955, Oppenheimer *et al.* (8) observed a lag period of 54 weeks after implantation of poly(methyl $[1-^{14}\text{C}]$ methacrylate) films into rats, until suddenly the excretion of radioactivity started and continued for 40 weeks. When the films were removed, the excretion of radioactivity disappeared. Schindler *et al.* (13) observed with polylactide implants that degradation of the polymer, measured by the decrease in the molecular weight via the viscosity of the implant, started soon after administration. The removal of material from the administration site, however, occurred only after a certain molecular weight was reached. After implantation of poly(ϵ -caprolactone-co-DL-lactic acid) capsules for instance, the viscosity decreased by 75%, while only 1% of the injected capsule material was removed from the injection site. Since the viscosity is directly related to the molecular weight, a comparable reduction of ~75% in the molecular weight has to be assumed. Over the following 8 weeks, the residual polymer disappeared totally from the site of administration, while the viscosity decreased only slowly.

A similar process possibly occurred after subcutaneous administration of poly(methyl $[1-^{14}\text{C}]$ methacrylate) nanoparticles and films. The deg-

radation might have started rather early after injection or implantation, but the removal from the site of administration and the excretion began only when a certain molecular weight of the degradation products was reached. The faster excretion rate during the first couple of days can also be explained by the limitation of the transportation and excretion process by the molecular weight. The initially excreted total amount of ~13% far exceeds the possible amount of residual monomers. As mentioned previously, $\leq 1\%$ residual monomers are contained in the polymer. However, as shown by gel permeation chromatography (14), the molecular weight distribution of the poly(methyl $[1-^{14}\text{C}]$ methacrylate) nanoparticles prepared by γ -irradiation is rather wide, allowing for a considerable amount of low-molecular weight polymer, some of which could be readily excreted.

REFERENCES

- (1) J. Kreuter and P. P. Speiser, *Infect. Immun.*, **13**, 204 (1976).
- (2) J. Kreuter, R. Mauler, H. Gruschkau, and P. P. Speiser, *Exp. Cell Biol.*, **44**, 12 (1976).
- (3) J. Kreuter and E. Liehl, *Med. Microbiol. Immunol.*, **165**, 111 (1978).
- (4) J. Kreuter and E. Liehl, *J. Pharm. Sci.*, **70**, 367 (1981).
- (5) J. Kreuter and I. Haenzel, *Infect. Immun.*, **19**, 667 (1978).
- (6) J. Kreuter, U. Täuber, and V. Illi, *J. Pharm. Sci.*, **68**, 1443 (1979).
- (7) L. Tomatis, *Tumori*, **52**, 165 (1966).
- (8) B. S. Oppenheimer, E. T. Oppenheimer, I. Danishefsky, A. P. Stout, and F. R. Eirich, *Cancer Res.*, **15**, 333 (1955).
- (9) A. Murray and D. L. Williams, "Organic Synthesis with Isotopes, Part I," Interscience, New York, N.Y., 1958.
- (10) P. Edman and I. Sjöholm, *J. Pharm. Sci.*, **70**, 684 (1981).
- (11) M. Barvic, K. Kliment, and M. Zaradil, *J. Biomed. Mater. Res.*, **1**, 313 (1967).
- (12) L. Sprincl, J. Kopecek, and D. Lim, *J. Biomed. Mater. Res.*, **4**, 447 (1971).
- (13) A. Schindler, R. Jeffcoat, G. L. Kimmel, C. G. Pitt, M. E. Wall, and R. Zweidinger, in "Contemporary Topics in Polymer Science," Vol. 2, E. M. Pearce and J. F. Schaeffgen, Eds., Plenum, New York, N.Y., 1977, pp. 251-289.
- (14) V. Bentele, U. E. Berg, and J. Kreuter, *Int. J. Pharm.*, **13**, 109 (1983).

Solid-State Decomposition of Alkoxyfuroic Acids in the Presence of Microcrystalline Cellulose

J. T. CARSTENSEN* and ROHIT C. KOTHARI*

Received April 9, 1982, from the School of Pharmacy, University of Wisconsin, Madison, WI 53706.

Accepted for publication August 24, 1982.

* Present address: Riker Laboratories, St. Paul, MN 55119.

Abstract □ A solid-solid interaction between alkoxyfuroic acids and microcrystalline cellulose has been studied. The decomposition of the mixture differs from that of the drug(s) alone, in that carbon monoxide (not carbon dioxide) is the high-temperature decomposition product. A model is proposed in which interaction occurs at contact points. A liquid decomposition product, dissolving part of the alkoxyfuroic acid (to the extent of its solubility) serves as a carrier, so that the number of contact points increases, thus accelerating the reaction. Both the main and ancillary parameters have calculated values that are consistent with the model.

Keyphrases □ Alkoxyfuroic acid—solid-state interactions with microcrystalline cellulose, decomposition model □ Microcrystalline cellulose—solid-state interactions with alkoxyfuroic acids, decomposition model □ Decomposition—alkoxyfuroic acids with microcrystalline cellulose, model, solid-state interactions

The interaction between solid drugs and solid excipients is of great theoretical and practical interest. Most studies

deal with multicomponent systems, but even when only two solid components are present, the presence of air complicates the interpretation of data. Nevertheless, good direct conclusions have frequently been derived (1, 2).

This study describes the interaction between a drug (5-alkoxy-2-furoic acid)¹ and a common pharmaceutical excipient (microcrystalline cellulose). Interactions between drugs and this excipient have been reported in the past (3) and present a challenging field of investigation.

EXPERIMENTAL

The 5-alkoxy-2-furoic acids were synthesized and purified as described by Carstensen and Kothari (4). The microcrystalline cellulose used² was

¹ A few studies were carried out with the C_8 derivative as well.

² Avicel; FMC Corp., West Point, Pa.